

# Deakin Research Online

*Deakin University's institutional research repository*

**This is the author's final peer reviewed version of the item published as:**

He, Wendy W. and Wang, Xungai 2004, Numerical modeling of the dynamic tensile behavior of irregular fibers, *Journal of applied polymer science*, vol. 91, no. 5, pp. 2855-2861.

**Copyright :** 2004, Wiley Periodicals, Inc.

# Numerical Modeling of the Dynamic Tensile Behavior of Irregular Fibers

Wendy W. He and Xungai Wang

School of Engineering & Technology  
Deakin University, Geelong VIC 3217 Australia

## Synopsis

Most fibers are irregular, and they are often subjected to rapid straining during mechanical processing and end-use applications. In this paper, the effect of fiber dimensional irregularities on the dynamic tensile behavior of irregular fibers is examined, using the finite element method (FEM). Fiber dimensional irregularities are simulated with sine waves of different magnitude (10%, 30% and 50% level of diameter variation). The tensile behavior of irregular fibers is examined at different strain rates (333%/sec, 3,333%/sec and 30,000%/sec). The breaking load and breaking extension of irregular fibers at different strain rates are then calculated from the finite element model. The results indicate that strain rate has a significant effect on the dynamic tensile behavior of an irregular fiber, and that the position of the thinnest segment along the fiber affects the simulation results markedly. Under dynamic conditions, an irregular fiber does not necessarily break at the thinnest segment, which is different from the quasi-static results.

## Keywords:

Fibers, irregularity, dynamic, stress, strain

## 1. INTRODUCTION

Fibers, yarns and even some fabrics are often subjected to high rate of straining during processing and applications. For instance, in a regular passenger-car tire traveling at 50 miles per hour, the cords are strained at a rate approached 1000%/sec, and the threads during stitching operation are also applied a high impact velocity of 10 m/sec<sup>1</sup>. In processes such as high speed carding, the individual fibres are also impacted upon at speeds exceeding 10 m/s. The impact velocity for ballistic fabrics is much higher still. Therefore, the study of the tensile behavior of textile materials under dynamic conditions is important.

Some papers have reported the tensile properties of textile materials at different strain rates. Meredith<sup>2</sup> measured the stress-strain relationships of rayon, silk and nylon yarns for several strain rates from 0.001%/sec to 1000%/sec, respectively. He found that with increasing rate of straining, the strength increased for all the yarns and the breaking extension increased for rayon and silk yarns but decreased for nylon at a higher strain rate. He also confirmed that the effect of strain rate on breaking extension was much smaller than its effect on strength. Holden<sup>3</sup> used a modified experimental apparatus to increase the strain rate to 66,000%/sec and obtained the data of breaking stress and breaking strain of different continuous-filament yarns. Hall<sup>4, 5, 6</sup> examined the stress-strain curves of different fibers and yarns at strain rates between 0.01%/sec and 33,000%/sec and reported that the breaking stress was high, but the breaking strain might be low or high with increasing the strain rate depending upon the materials tested, which

is consistent with the results obtained by Smith *et al*<sup>7</sup>. In recent years, there is interest in the tensile behavior of fiber-reinforced composites at different strain rates. Wang and Xia<sup>8</sup> established the relationships of the glass fiber strength and six different strain rates using bimodal Weibull distribution. Mano and Viana<sup>9</sup> and Wang *et al*<sup>10</sup> carried out the tensile stress-strain experiments in a glass fiber reinforced polyamide-6 composite at different strain rates and Gilat *et al*<sup>11</sup> also examined a carbon/epoxy composite in this aspect. They all reported similar results, namely, the strength of composite increased markedly with increasing strain rate, but the extension would decrease slightly except for  $\pm 45^\circ$  laminate composite<sup>11</sup>. A modified Weibull distribution has also been developed for fibers with dimensional irregularities along fiber length<sup>12</sup>. However, little is available in the research literature on the effect of fiber diameter irregularities on the dynamic tensile properties of irregular single fibers.

We have applied the finite element method (FEM) to investigate the quasi-static tensile behavior of fibers with dimensional irregularities<sup>13, 14</sup>. In this paper, we use this technique with the ABAQUS (Version 6.3)<sup>15, 16</sup> software package to simulate dimensional irregularities of single fibers and analyze their tensile behavior at high straining rates.

## **2. FINITE-ELEMENT MODEL**

### **2.1 Assumptions of fiber specimen**

In this study, we ignore any internal structure variability of the fiber specimen and consider only the fiber dimensional irregularity along the fiber length. We also assume that the fiber cross-section is circular and the fiber is axisymmetric, so that fiber diameter variation can represent its dimensional irregularity. The different fiber diameter variations follow the sine wave pattern in all the simulations below. The material is strain rate dependent and its tensile behavior (stress-strain curves) is given by Lyons<sup>1</sup> in Figure 1. In the simulation, the data of static curve is used for ABAQUS input, and the rate-dependent curves are then expressed in terms of the static relation. Relevant parameters concerning the fiber specimen are listed in Table 1.

Table 1. The parameters of the fiber specimen

Properties		Value
Young's modulus (MPa)		8160
Poisson's ratio		0.35
Density ( $g/cm^3$ )		0.95
Static true stress at break (MPa)		697
Strain rate dependence	Yield stress ratio	3.0
	Equivalent plastic strain rate	300
Specimen diameter ( $\mu m$ )		20
Specimen length (mm)		0.5

## 2.2 Description of the Finite Element Model

The non-linear finite element analysis is used in this study. We model the fiber specimen as a three-dimensional (3D) solid structure using C3D8R elements. The shape of

elements in the model is cuboid. There are eight nodes on each element, one on each corner of the cube. In the analysis, one end (left) of the fiber specimen is fixed, the other end (right) is extended along the fiber length at different strain rates until the fiber specimen reaches the maximum tensile stress (true stress at break at the corresponding strain rate) and breaks. Figure 2 gives an example of the finite element mesh of the fiber specimen.

### **2.3 Determination of the number of elements or mesh density**

It is important that an adequate mesh is used to ensure that the results from the ABAQUS simulation are accurate. Coarse meshes can yield inaccurate results and very fine meshes require more computing time. It is therefore necessary to determine the appropriate number of elements (mesh density) needed for a particular problem.

Here we perform a mesh convergence study using information given in Sections 2.1 and 2.2. The fiber specimen is analyzed with different mesh densities and we consider the influence of the number of elements on the fiber breaking load at a strain rate of 30,000%/sec. The results from the model are depicted in Figure 3, which shows that the variation of breaking load is less than 0.1% when the number of elements is greater than 7040/0.5mm. In other words, the simulation model at this mesh density will produce an accurate solution. Therefore, we have chosen a mesh density of 7040/0.5mm of fiber specimen for all simulations - the models are meshed by dividing them into 44 elements in cross-section area [(see Figure 2 (c))] and a total of 160 layers along the fiber specimen length (0.5mm) [(see Figure 2 (a) and (b))].

### **3. RESULTS AND DISCUSSION**

#### **3.1 Verification of the finite-element model**

In order to investigate the effect of fiber non-uniformity on fiber dynamic tensile behavior, we need to know the tensile behavior of the fiber without any structural and dimensional irregularities at a range of different strain rates. Here, we choose a group of stress-strain curves obtained at different strain rates for the polyethylene fiber<sup>1</sup>. In the model, we only simulate three different strain rates— $2 \times 10^4$  %/min (333%/sec),  $2 \times 10^5$  %/min (3,333%/sec) and  $1.8 \times 10^6$  %/min (30,000%/sec)<sup>1</sup>. In addition, 10%/min (0.167%/sec) is regarded as quasi-static rate (<3.3%/sec) and the data from its stress-strain curve are supplied to define the characteristics of material in ABAQUS. A comparison between the results obtained from experiments<sup>1</sup> and those from FE model is shown in Figure 4. We found a similar trend in both breaking load and breaking extension between the experimental and modeling results, with a relatively small discrepancy. This discrepancy may be due to the assumption – cross section is circular and uniform along the fiber length – which may not be strictly the case for the polyethylene fibers used in the previous experiments<sup>1</sup>. Nevertheless, the agreement between the two sets of data is good, and the FE model can be acceptable for the simulation work that follows.

#### **3.2 Effect of level of variation on fiber dynamic tensile properties**

We simulate two different cases here [Case 1 and Case 2 in Table 2]. Case 1 represents a uniform fiber specimen with a diameter of 20  $\mu\text{m}$  and a length of 0.5 mm (a short

specimen length is used to save computation time). Case 2 simulates the irregular fiber with the same average diameter and length but with 10%, 30% and 50% levels of diameter variation, respectively, which are represented by a complete sine wave, and the thinnest segment (A) along the fiber is near the right end (the end of force application) in each fiber specimen [Figure 2 (a), 30% level of variation only]. In the simulation model, we also applied a strain rate of 333%/sec, 3,333%/sec and 30,000%/sec to these fiber specimens, respectively. Table 2 lists the results from the FE model.

The results indicate that for a fixed strain rate, an increase in the level of diameter variation leads to a reduction in the breaking load and breaking extension. As the minimum fiber segment is close to the end of force application along the fiber, the maximum stress propagates to or near the thinnest segment of the fiber during fiber extension. A graphical depiction of stress distribution of these cases is illustrated in Figure 5. As the level of irregularity increases, the minimum fiber diameter decreases, the fiber therefore weakens. Figure 6 shows the load-extension curves of fiber specimens with different levels of diameter variation extended at a strain rate of 3,333%/sec. The results are also consistent with early experimental results<sup>17</sup> and our quasi-static modeling results<sup>13, 14</sup>. However, when the strain rate increases, there is a significant increase in the breaking load and a slight decrease in the breaking extension of the fiber for three different levels of variation. This is consistent with the experimental results obtained in previous studies<sup>2, 9</sup>. The load-extension curves of fiber specimens with 30% level of diameter variation at different strain rates are given in Figure 7.

### **3.3 Effect of position of the thin segment on fiber dynamic tensile properties**

As indicated in Table 2, we simulate three different cases (Case 3, Case 4 and Case 5). Their simulation conditions are the same as the Case 2, but the thinnest segment (B) along the fiber is away from the right end (the end of force application) in each case [Figure 2 (b), 30% level of variation only]. In the model, we applied a strain rate of 333%/sec and 30,000%/sec to the fiber specimens. The simulation results from the FE model are listed in Table 2.

When the fiber is extended, we find that its breaking load increases and its breaking extension decreases with increasing strain rate for a given level of diameter variation. However, for a given strain rate, the higher the level of diameter variation, the higher the breaking load and the lower the breaking extension. For a dynamic tensile behavior analysis, we should consider the stress propagation along the fiber specimen. Figure 8 shows the propagation of stress in the fiber at successive extensions during the simulation for Case 4 at the strain rate of 333%/sec. We observe that the maximum stress in fiber specimen does not propagate to the thinnest segment along the fiber when the fiber is extended but concentrates on the relatively coarse end. As the level of diameter variation increases, the maximum fiber diameter increases (for a given average fiber diameter) and the fiber will be able to sustain increased load. This leads to increased fiber breaking load and reduced fiber breaking extension. In fact the breaking load is even higher than that of the uniform fiber at the same strain rate (Case 3, 4, 5 and Case 1 in Table 2). In other words, the significant result here is that the breakage of fiber does not always occur at the thinnest segment along the fiber under dynamic tensile conditions, which is

obviously different from the static analysis. It is worth noting that the effect of position of the thinnest segment on the fiber dynamic tensile behavior is more marked at a higher level of diameter variation than that at a lower level of diameter variation, which is shown in Figure 9.

#### **4. CONCLUSIONS**

A three-dimensional (3D) finite-element model has been utilized to investigate the dynamic tensile behavior of fiber specimens with simulated dimensional irregularities.

The following conclusions can be drawn from this study:

.

- The level of diameter variations significantly influences the dynamic tensile behavior of the fiber. As the level of variation increases, the breaking load and breaking extension decrease at different strain rates. At a fixed level of diameter variation, the higher the strain rate, the higher the breaking load, but the lower the breaking extension.
- For a dynamic tensile behavior analysis, the propagation of stress wave in the fiber specimen is important and the fiber does not necessarily break at its thinnest segment. The position or distribution of the thinnest fiber segment along the fiber length has a significant influence on the dynamic tensile behavior of the fiber. When the thinnest segment along the fiber is far away from the end of force application, the fiber specimen has a high breaking load and a low breaking extension, and the breaking load of such an irregular fiber is even higher than that of a uniform fiber under the

same simulation conditions. This is an important difference from the results obtained under quasi-static conditions.

## Literature Cited

1. W. J. Lyons, Impact Phenomena in Textiles, Chapter 6, p127. *The M. I. T. Press*, Cambridge, Massachusetts, 1963
2. R. Meredith, The Effect of Rate of Extension on the Tensile Behaviour of Viscose and Acetate Rayons, Silk and Nylon, *J. Textile Inst.*, **45**, T30-43, 1954
3. G. Holden, Tensile Properties of Textile Fibres at Very High Rates of Extension, *J. Textile Inst.*, **50**, T41-54, 1959
4. H. Hall, The Effect of Temperature and Strain Rate on the Stress-strain Curve of Oriented Isotactic Polypropylene, *Journal of Polymer Science*, **54**, 505-522, 1961
5. H. Hall, The Tensile Properties of Textile Yarns at High Strain Rates, *Journal of Applied Polymer Science*, **8**, 237-256, 1964
6. H. Hall, The Effect of Strain Rate on the Stress-strain Curves of Oriented Polymers. I: Presentation of Experimental Results, *Journal of Applied Polymer Science*, **12**, 731-738, 1968
7. J. C. Smith, P. J. Shouse, J. M. Blandford, and K. M. Towne, Stress-Strain Relationships in Yarns Subjected to Rapid Impact Loading. Part VII: Stress-strain Curves and Breaking Energy Data for Textile Yarns, *Textile Res. J.*, 721-734, 1961
8. Z. Wang, and Y. Xia, Experimental Evaluation of the Strength Distribution of Fibers under High Strain Rates by Bimodal Weibull Distribution, *Composites Science and Technology*, **57**, 1599-1607, 1997
9. J. F. Mano, and J. C. Viana, Effects of the Strain Rate and Temperature in Stress-strain Test: Study of the Glass Transition of a Polyamide-6, *Polymer Testing*, **20**, 937- 943, 2001

10. Z. Wang, Y. Zhou, and P. K. Mallick, Effect of Temperature and Strain Rate on the Tensile Behavior of Short Fiber Reinforced Polyamide-6, *Polymer Composites*, **23** (5), 858-871, 2002
11. A. Gilat, R. K. Goldberg, and G. D. Roberts, Experimental Study of Strain-rate-dependent Behavior of Carbon/epoxy Composite, *Composites Science and Technology*, **62**, 1469-1476, 2002
12. Y. P. Zhang, X. Wang, N. Pan, and R. Postle, Weibull Analysis of the Tensile Behavior of Fibers with Geometrical Irregularities, *J. Materials Sci.*, Vol 37, No 7, pp1401-1406, 2002
13. W. He, S. Zhang, and X. Wang, Mechanical Behavior of Irregular Fibers – Part 1: Modelling the Tensile Behavior of Linear Elastic Fibers, *Textile Res. J.*, **71** (6), 556-560, 2001
14. W. He, X. Wang, and S. Zhang, Mechanical Behavior of Irregular Fibers – Part 2: Non-linear Tensile Behavior, *Textile Res. J.*, **71**(11), 939-942, 2001
15. ABAQUS, *ABAQUS/Explicit User's Manual*, Version 6.3 Hibbitt, karlsson & Sorensen, Inc. U.S.A., 2002
16. ABAQUS, *ABAQUS/CAE User's Manual*, Version 6.3 Hibbitt, karlsson & Sorensen, Inc. U.S.A., 2002
17. Y. P. Zhang, and X. Wang, The Effect of Along-fibre Diameter Variation on Fiber Tensile Behavior, *Wool Technology and Sheep Breeding*, **48** (4), 303-312, 2000

## List of figures

Figure 1: Stress-strain curves of polyethylene fibers at various strain rates

Figure 2: 3D finite element mesh used for analyzing the dynamic fiber tensile behavior

Figure 3: The breaking force versus number of elements (strain rate of 30,000%/sec)

Figure 4: Comparison of the simulation results from FE model and experimental results obtained by Lyons under quasi-static condition and at three different strain rates

Figure 5: A graphical depiction of stress distribution of Case 2 at the strain rate of 3,333%/sec

Figure 6: Load-extension curves for fiber specimen with different levels of diameter variation (strain rate of 3,333%/sec)

Figure 7: Load-extension curves for fiber specimen at different strain rates (30% levels of diameter variation used)

Figure 8: The contours of the stress in a fiber during successive extensions for Case 4 at the strain rate of 333%/sec

Figure 9: Load-extension curves for fiber with different diameter variation and position of the thinnest segment at the strain rate of 30,000%/sec

Table 2 : Data for fiber specimen with different diameter variations  
at different strain rates

Simulation Cases	Simulation Conditions			Simulation Results	
	Position of the thinnest segment	Level of variation (%)	Strain rate (%/sec)	Breaking load (g)	Breaking extension (%)
Case 1	-	0 (uniform)	333 3,333 30,000	30.27	5.30
				34.33	4.34
				38.23	3.97
Case 2	A	10		21.94	3.69
				32.76	3.50
				36.76	3.36
		30		17.74	3.42
				28.73	3.30
				33.08	3.24
		50	14.64	3.11	
			18.05	3.03	
			21.76	2.90	
Case 3	B	10	333 30,000	30.64	3.49
38.89				3.26	
Case 4		30		31.75	3.20
40.28				2.93	
Case 5		50		33.43	2.77
				41.45	2.65

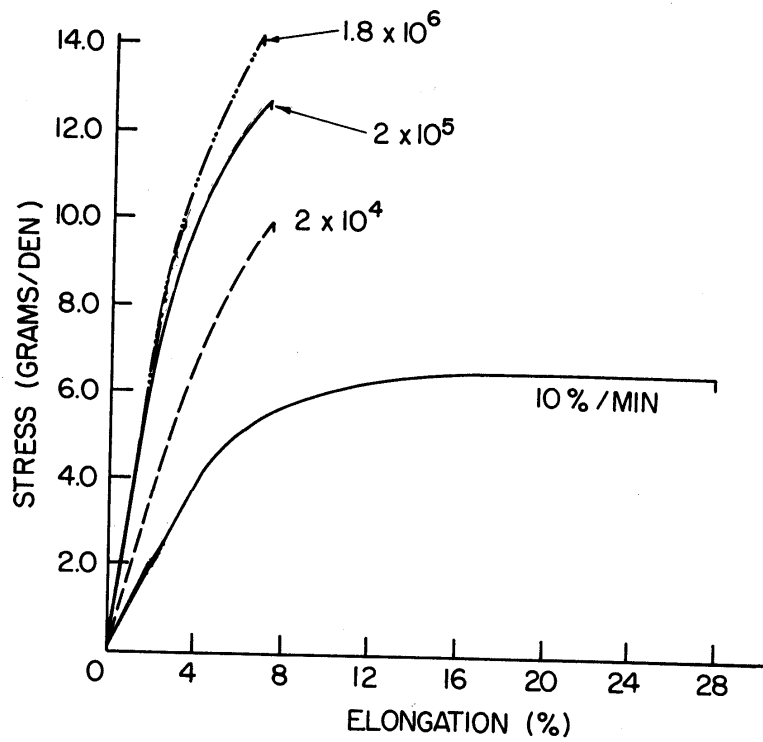


Figure 1: Stress-strain curves of polyethylene fibers at various strain rates <sup>1</sup>

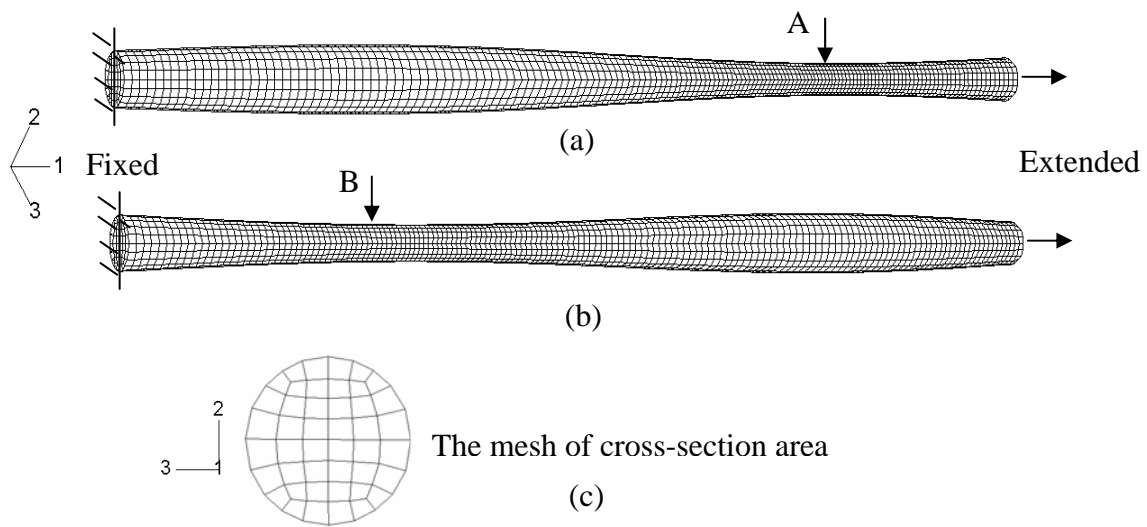


Figure 2: 3D finite element mesh used for analyzing the dynamic fiber tensile behavior

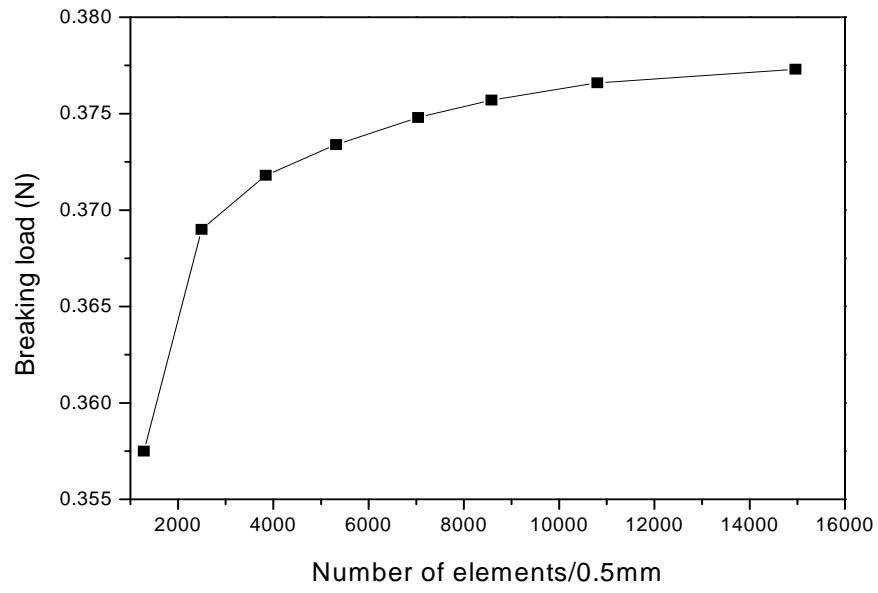


Figure 3: The breaking load versus number of elements (strain rate of 30,000%/sec)

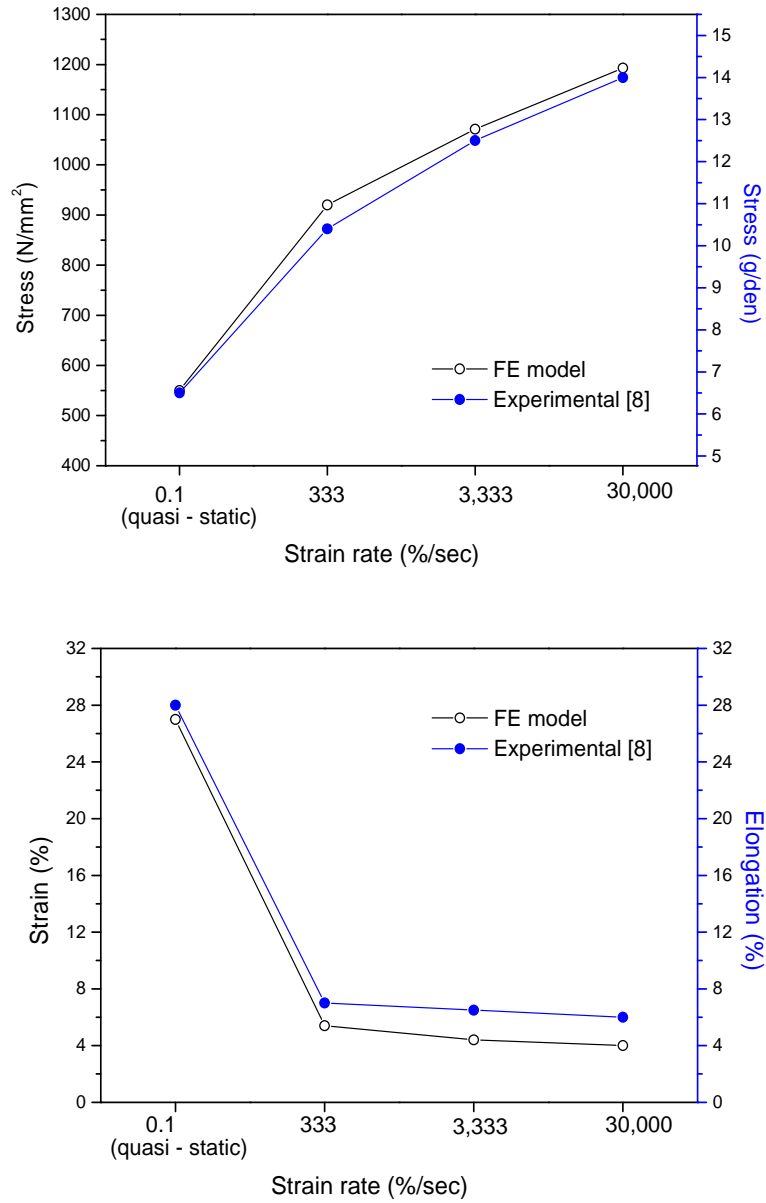


Figure 4: Comparison of the simulation results from FE model and experimental results obtained by Lyons under quasi-static condition and at three different strain rates

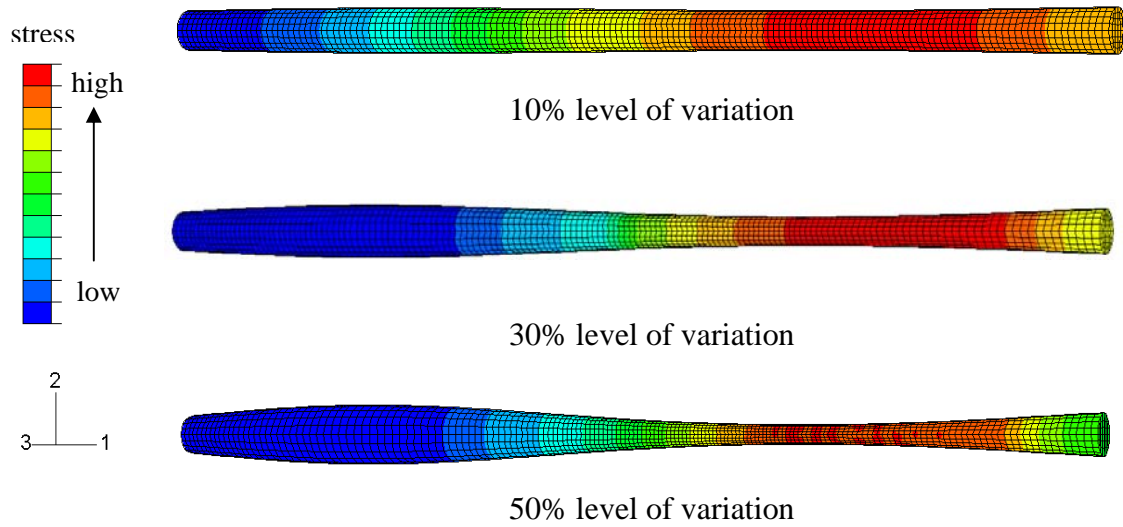


Figure 5: A graphical depiction of stress distribution of Case 2  
at the strain rate of 3,333%/sec

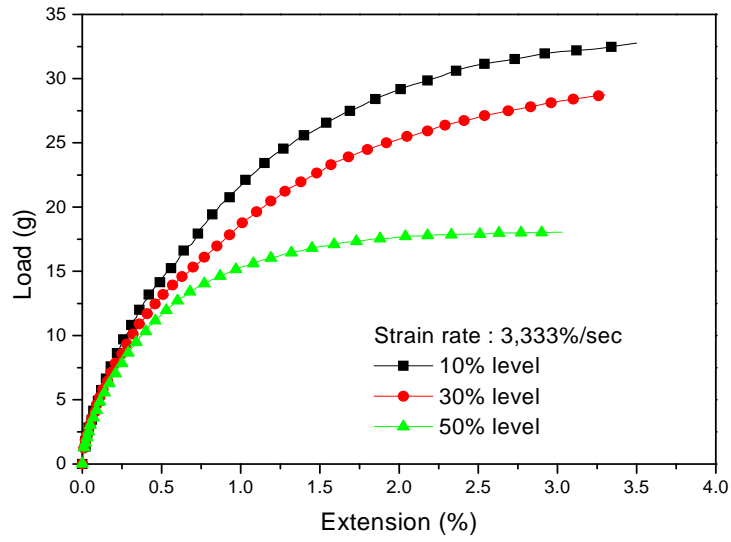


Figure 6: Load-extension curves for fiber specimen with different levels of diameter variation (strain rate of 3,333%/sec)

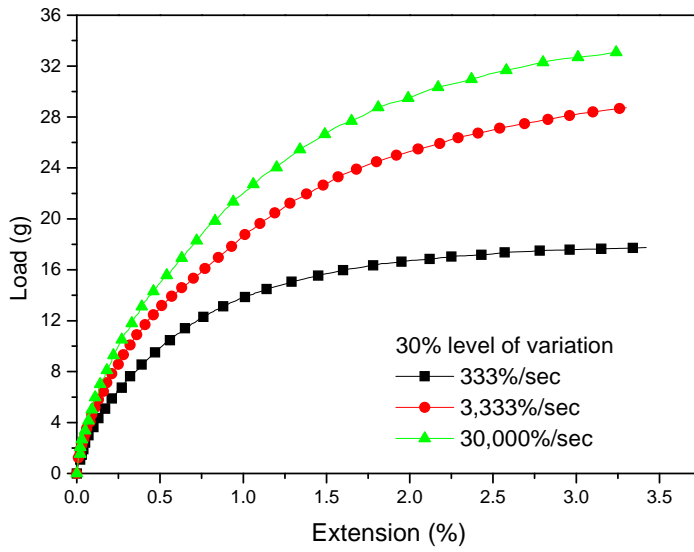


Figure 7: Load-extension curves for fiber specimen at different strain rates  
(30% levels of diameter variation used)

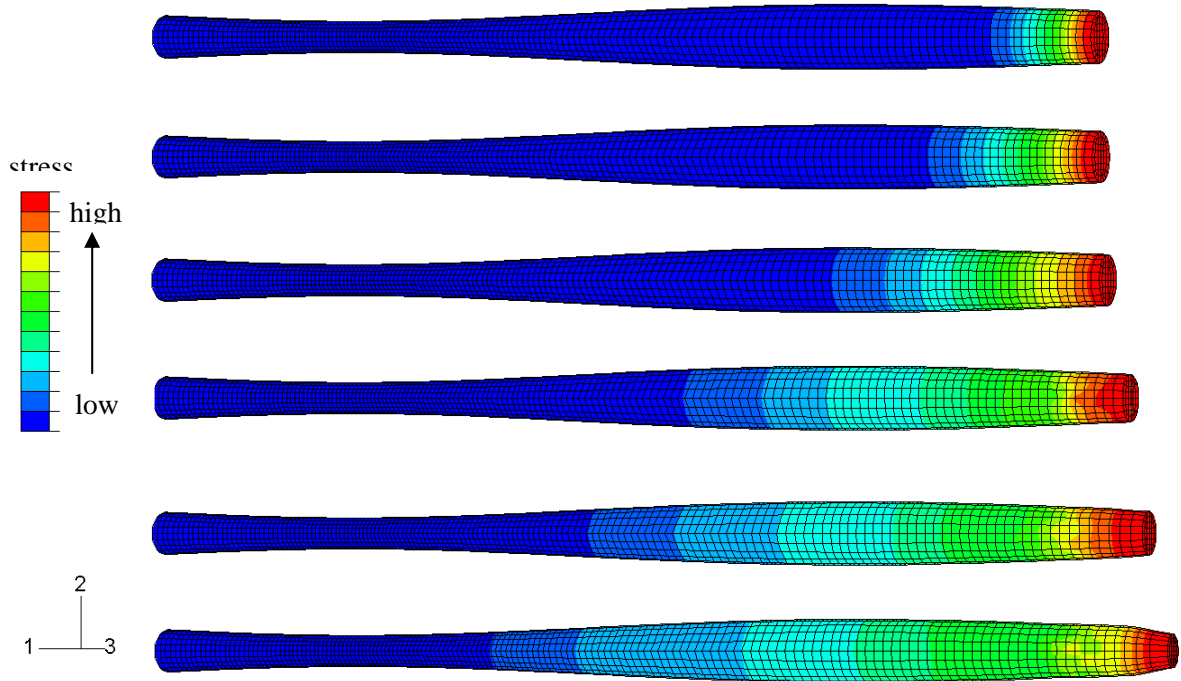


Figure 8: The contours of the stress in a fiber during successive extensions  
for Case 4 at the strain rate of 333%/sec

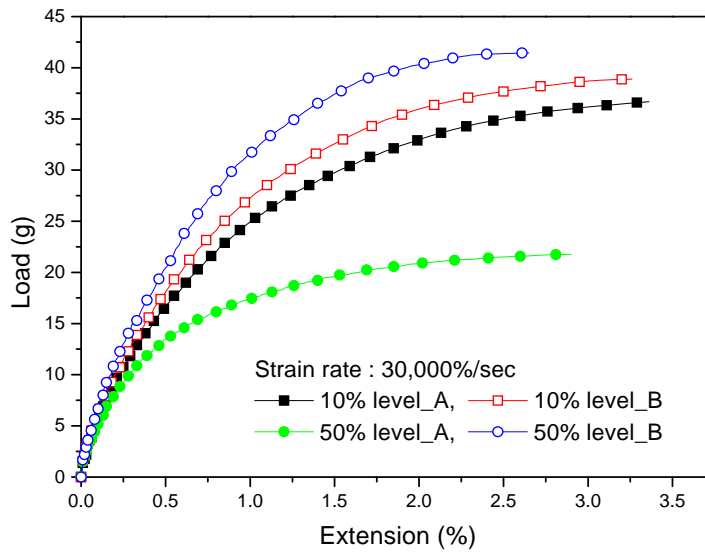


Figure 9: Load-extension curves for fiber with different diameter variation and position of the thinnest segment at the strain rate of 30,000%/sec